Research on CLLLC Resonant Bidirectional DC-DC Converter

Research on CLLLC Resonant Bidirectional DC-DC Converter

Hou Lei[1,3], Ma Huizhuo[1], Chen Xingyu[2] and Zhang Kang[1]

[1]State Grid Hebei Electric Power Co., Ltd. Xiong an New Area Power Supply Company, Baoding, China
[2]XJ Group Corporation, Xuchang, China

[3]**13983943@qq.com**

Abstract. Based on the single-phase full-bridge LLC DC-DC converter, the LC series resonant network is introduced in the secondary side of the high frequency transformer to form the bidirectional CLLLC resonant DC-DC converter. Firstly, the bidirectional CLLLC resonant DC-DC converter was used for mathematical modeling. By extending the description function, the large-signal steady-state model of the converter was obtained, and the DC voltage gain when the DC-DC converter was running forward was deduced. The gain characteristics and frequency characteristics of the model are compared with those of the basic wave equivalent model. Secondly, the small-signal perturbation model of CLLLC DC-DC converter is modeled, and the small-signal perturbation is brought into the large-signal steady-state solution to obtain the transfer function when the CLLLC resonant converter is running forward. Finally, a 20kW CLLLC DC-DC converter is designed, and the simulation analysis is carried out to verify the correctness of the proposed scheme.

1. Introduction

With the increasing demand for natural resources in society, the active exploration of renewable energy is the most effective method to solve the energy crisis in view of the shortage of primary energy[1-3].New energy technology is becoming the main force to promote the development of renewable energy[4].In order to solve the energy problem, the bidirectional isolation DC-DC converter has a wide application prospect in the fields of distributed energy generation, micro-grid, DC distribution network, electric vehicle and uninterrupted power supply system[5].

Isolated bidirectional DC-DC converter can realize the bidirectional flow of energy. At present, a relatively mature (Dual Active Bridge, DAB) topology consists of two H-bridges and a high-frequency isolation transformer[6]. However, the voltage gain range of the dual active bridge structure is narrow, and when the voltage of the input end and the output end do not match, the ZVS characteristic will be lost and large back-flow power will be generated, which reduces the efficiency[7]. On this basis, a series of bidirectional full-bridge resonant DC-DC converters have evolved[8-9]. According to the number of resonant cavity components of the resonant converter, it is mainly divided into two components: series resonant SRC and parallel resonant PRC resonant converters; LCC and LLC Three-element Resonant Converter[10]; CLLC and LLCL Four-element Resonant Converter[11]; CLLLC five-element resonant converter[12].The two-element resonant and three-element resonant structures are asymmetrical, and when the energy flows in the opposite direction, the operating characteristics and soft switching characteristics are different, so the design of control strategy and resonance parameters is more

complex[13].A resonant inductor or capacitor is added to the secondary side of the three-element resonant cavity transformer to form the four-element resonant symmetric converter. The symmetric topology can ensure that the converter has the characteristics of LLC soft switching when it is running in both the forward and reverse directions[14].
In this paper, CLLLC resonant converter is taken as the research object. Based on the LLC converter, a series LC resonant slot is added on the secondary side of the high frequency transformer and its resonant parameters are designed and symmetrical with those on the primary side, forming a two-way LLC resonant topology[15]. Literature [16] introduces the working process of CLLLC resonant converter. Forward and reverse operation is similar to full-bridge LLC converter operation state.

2. Operating principle of CLLLC resonant converter

The topology of the CLLLC resonant converter is shown in Figure 1, which can be divided into two parts. The four IGBTs at the front stage constitute the inverter unit, and the four IGBTs at the rear stage constitute the rectification unit. C_{in}, C_0 is the filter capacitor in positive and negative operation; L_1, C_1 are resonant inductor and resonant capacitor respectively; L_m is the excitation inductance of the transformer; L_2, C_2 is the resonant inductor and resonant capacitor of the last stage. When the resonance parameters design, will rank after the resonant inductor design for $L_2 = L_1/n^2$, $C_2 = n^2 C_1$,where n variable than for transformer, make CLLLC converter topology is completely symmetrical.

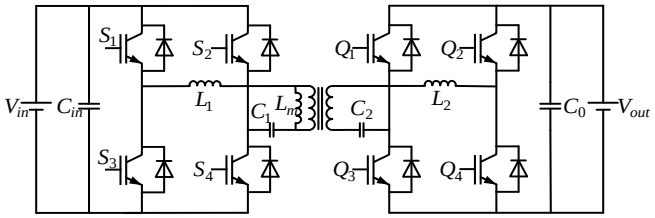

Figure 1. Topology of bi-directional CLLLC resonant converter

When the CLLLC resonant converter is running forward, the primary side is the high voltage side, the switch tube $S_1 \sim S_4$ switch tube is supplemented with complementary drive signals, and the latter stage is rectified through the body diode of the switch tube. When the secondary side is the reverse operation of the low-voltage side, the switch tube $Q_1 \sim Q_4$ switch tube is supplemented with complementary drive signals, and the rectifier side is uncontrolled rectifier, which can realize the bidirectional transmission of energy [17]。Sf literature [18] in converter work frequency f_s and the relationship between the size of the resonance frequency f_r points will be resonant converter is divided into three kinds of working state and: $f_s < f_r$ owe resonance state; $f_s = f_r$ quasi resonant state; $f_s > f_r$ harmonic state three work modes. Literature [19] points out that in order to obtain the maximum voltage gain, the converter generally operates in under resonant or quasi-resonant state by setting the resonant parameters of the multi-pass pair. At present, the main analysis method of resonant converter is the fundamental wave approximation FHA method, which is only used in the analysis near the resonant frequency. When the converter's working frequency is offset, FHA method has a large error [20]. Literature [21] analyzed the resonant converter in time domain by using the method of synchronous PWM fixed frequency and duty cycle adjustment, but the PWM modulation method has a small variable voltage gain and is not suitable for wide voltage gain. The Particle Swarm Optimization (PSO) algorithm in Literature [22] is used to model the LLC converter, but the PSO algorithm is too complex to be suitable for practical application.

3. Mathematical modeling of CLLLC resonant converter

The state space averaging method is usually used to analyze the resonant converter with PWM control mode. In order to obtain wider voltage gain and further reduce switching loss, the CLLLC resonant converter adopts PFM pulse frequency modulation. The use of PFM frequency conversion control no

longer meets the premise of PWM modulation small ripple hypothesis, and the state-space average method is no longer applicable to frequency conversion control[23]. Literature [24] proposes a control method of equivalent circuit model, but its working process for resonant converter is complicated, and the forward and reverse operation transfer function cannot be obtained. In Literature [25], the extended description function method was used to model and analyze the LLC converter. In this paper, the extended description function is used to analyze the large-signal steady-state model of the bidirectional CLLLC resonant converter, and on this basis, the small-signal model of the CLLLC resonant converter is established and the resonant cavity parameters are designed and calculated [26].
It is assumed that the waveform of the resonant cavity element is approximately sinusoidal and the IGBT switch tube is an ideal device. The influence of parasitic capacitance is very small and does not affect the normal state of the resonant frequency operating point.

3.1 Establishment of Stat

The input voltage V_{in} can be equivalent to the high-frequency square-wave AC voltage at the output end of the full-bridge inverter circuit through the filter capacitor. The square wave voltage with the same amplitude as the input voltage is used to replace the input voltage of the resonator in the equivalent circuit. The rectifier side is replaced by a controlled voltage source. Its equivalent model is shown in Figure 2:

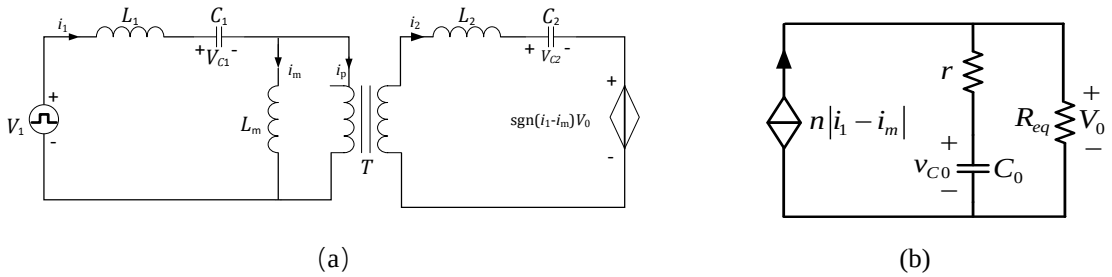

Figure 2. CLLLC resonant converter equivalent model

In V_{in} Figure 2(a) for the replacement of square wave voltage and equivalent for the size of the input voltage rectifier side $\mathrm{sgn}(i_1-i_m)v_0$ controlled voltage source. In Figure 2(b) transformer output equivalent to size of $n|i_1-i_m|$ controlled current source, output equivalent resistance as the R_{eq}, output filter capacitor of series resistance. According to Kirchhoff's voltage and current law, the nonlinear state of the CLLLC resonant converter is as follows:

$$\begin{cases} V_1 = L_1\dfrac{di_1}{dt} + v_{C1} + L_m\dfrac{di_m}{dt} \\ L_m\dfrac{di_m}{dt} = n\left[L_2\dfrac{d\left(i_1-i_m\right)}{dt} + v_{C2} + \mathrm{sgn}\left(i_1-i_m\right)v_0\right] \\ V_0 = R'n\left|i_1-i_m\right| + R'v_{C0}/r \\ n\left|i_1-i_m\right| = \left(1+\dfrac{r}{R_{eq}}\right)C_0\dfrac{dv_{C0}}{dt} + \dfrac{v_{C0}}{R_{eq}} \\ i_1 = C_1\dfrac{dv_{C1}}{dt} \\ n\left(i_1-i_m\right) = C_2\dfrac{dv_{C2}}{dt} \end{cases} \tag{1}$$

Type of sgn as symbolic function, $i_1 - i_m$ plus or minus represent the flow of electric current, when $i_1 - i_m > 0$, $i_1 - i_m = 1$ said synthetic reference voltage and current; When $i_1 - i_m < 0$, $i_1 - i_m = -1$ said against to the reference voltage and current. $|i_1 - i_m|$ to the absolute value of $i_1 - i_m$ only on behalf of the direction is always the same size[27]. $R^{'} = rR_{eq}/(r + R_{eq})$ series parallel connection of equivalent resistance and load equivalent resistance value.

3.2 Extended Harmonic Approximation Analysis

When the CLLLC resonant converter works, the switching angular frequency is set as, and the current flowing through the resonant element and the voltage of the resonant element are approximately sine waves. According to the theory of frequency modulation signal, when the resonant converter is disturbed, the input square wave voltage of the resonant tank can be represented by the superposition of a time-varying amplitude sine signal and cosine signal during the adjustment of the system. According to the extension function theory, the resonant element voltage v_{C1}, v_{C2}, and resonant current i_1, i_m and i_2 variables are carried out corresponding superposition linear processing of sinusoidal signals and cosine signals. That is:

$$\begin{cases} i_1(t) = i_{1s}\sin(\omega_s t) + i_{1c}\cos(\omega_s t) \\ i_m(t) = i_{ms}\sin(\omega_s t) + i_{mc}\cos(\omega_s t) \\ i_2(t) = n\begin{bmatrix} i_{1s}(t) - i_{ms}(t)\sin(\omega_s t) \\ +\left(i_{1c}(t) - i_{mc}(t)\right)i_{mc}\cos(\omega_s t) \end{bmatrix} \\ v_{C1}(t) = v_{C1s}(t)\sin(\omega_s t) + v_{C1c}(t)\sin(\omega_s t) \\ v_{C2}(t) = v_{C2s}(t)\sin(\omega_s t) + v_{C2c}(t)\sin(\omega_s t) \end{cases} \tag{2}$$

Derivation of nonlinear variables in (2) is taken and the harmonic approximate state expression of nonlinear variables is obtained by sorting out:

$$\begin{cases} \frac{di_1}{dt} = \left(\frac{di_{1s}}{dt} - \omega_s i_{1c}\right)\sin(\omega_s t) + \left(\frac{di_{1c}}{dt} + \omega_s i_{1s}\right)\cos(\omega_s t) \\ \frac{di_m}{dt} = \left(\frac{di_{ms}}{dt} - \omega_s i_{mc}\right)\sin(\omega_s t) + \left(\frac{di_{mc}}{dt} + \omega_s i_{ms}\right) \\ \qquad \cos(\omega_s t) \\ \frac{di_2}{dt} = n\left[\left(\frac{di_{1s}}{dt} - \frac{di_{ms}}{dt} - \omega_s\left(i_{1c} - i_{mc}\right)\sin(\omega_s t)\right) + \right. \\ \qquad \left.\left(\frac{di_{1c}}{dt} - \frac{di_{mc}}{dt} + \omega_s\left(i_{1s} - i_{mc}\right)\cos(\omega_s t)\right)\right] \\ \frac{dv_{C1}}{dt} = \left(\frac{dv_{C1s}}{dt} - \omega_s v_{C1c}\right)\sin(\omega_s t) + \left(\frac{dv_{C1s}}{dt} + \right. \\ \qquad \left.\omega_s v_{C1c}\right)\cos(\omega_s t) \\ \frac{dv_{C2}}{dt} = \left(\frac{dv_{C2s}}{dt} - \omega_s v_{C2c}\right)\sin(\omega_s t) + \left(\frac{dv_{C2s}}{dt} + \right. \\ \qquad \left.\omega_s v_{C2c}\right)\cos(\omega_s t) \end{cases} \tag{3}$$

3.3 Establishment of Extended Description Functions

By the state of the (1) can see contains three nonlinear varia $\mathrm{nsgn}(i_1 - i_m)v_0$ and $n|i_1 - i_m|$ fundamental wave approximation using extended describing function, and that is:

$$\begin{cases} V_1 \approx f_1(d,V_{in})\sin(\omega_s t) \\ n\,\mathrm{sgn}(i_1-i_m)v_0 \approx nf_2(i_{1s}-i_{ms},i_{1c}-i_{mc})\sin(\omega_s t) \\ \qquad\qquad +nf_3(i_{1s}-i_{ms},i_{1c}-i_{mc})\cos(\omega_s t) \\ n|i_1-i_m| \approx nf_4(i_{1s}-i_{ms},i_{1c}-i_{mc}) \end{cases} \tag{4}$$

where, d is the duty cycle of the resonant converter; $f_1(d,V_{in})$ is equivalent square wave voltage amplitude of fundamental component; $f_2(i_{1s}-i_{ms},i_{1c}-i_{mc})$, $f_3(i_{1s}-i_{ms},i_{1c}-i_{mc})$ respect-ively for the output voltage of the sinusoidal component amplitude, cosine component amplitude; $f_4(i_{1s}-i_{ms},\ i_{1c}-i_{mc})$ extension describing function for output current. Fourier decomposition of (4) is performed to take the fundamental wave component and the following can be obtained:

$$\begin{cases} f_1(d,V_1)=\dfrac{4V_{in}}{\pi}\sin\left(\dfrac{\pi}{2}d\right) \\ f_2(i_{1s}-i_{ms},i_{1c}-i_{mc})=\dfrac{4}{\pi}\dfrac{(i_{1s}-i_{ms})}{X_i}v_0 \\ f_3(i_{1s}-i_{ms},i_{1c}-i_{mc})=\dfrac{4}{\pi}\dfrac{(i_{1c}-i_{mc})}{X_i}v_0 \\ f_4(i_{1s}-i_{ms},i_{1c}-i_{mc})=\dfrac{2}{\pi}X_i \end{cases} \tag{5}$$

Type, $X_i=\sqrt{(i_{1s}-i_{ms})^2+(i_{1c}-i_{mc})^2}$ said current component synthesis coefficient.

3.4 Large Signal Model Analysis of CLLLC Resonant Converter

Steady large signal model, first of all, the above (5) into the (4) extension description is obtained, then the results and (3) and (2) the expression of together into the (1) the nonlinear state, the nonlinear state variables of the sine and cosine components corresponding coefficient respectively are equal, the resulting harmonic balance. Based on the harmonic balance, the steady-state solution of CLLLC resonant converter is derived, and the steady-state large-signal model is established, and the steady-state solution is

$$\begin{cases} -2\pi f_s L_1 i_{1C}+v_{C1C}-2\pi f_s L_m i_{mC}=\dfrac{4}{\pi}V_{in}\sin\left(\dfrac{\pi}{2}d\right) \\ 2\pi f_s L_1 i_{1S}+v_{C1S}+2\pi f_s L_m i_{mS}=0 \\ R_{ac}i_{1S}-2\pi n f_s L_2 i_{1C}-R_{ac}i_{mS}+2\pi f_s(L_m+nL_2)i_{mC} \\ +nv_{C2S}=0 \\ 2\pi n f_s L_2 i_{1S}+R_{ac}i_{1C}-2\pi f_s(L_m+nL_2)i_{mS}-R_{ac}i_{mC} \\ +nv_{C2C}=0 \\ \dfrac{v_{C0}}{R_{eq}}=\dfrac{2n}{\pi}X_i \\ V_0=\dfrac{2}{\pi}nR'X_i+R'v_{C0}/r \\ ni_{1S}-ni_{mS}+2\pi f_s v_{C2C}=0 \\ ni_{1C}-ni_{mC}+2\pi f_s v_{C2S}=0 \\ i_{1S}+2\pi f_s C_1 v_{C1C}=0 \\ i_{1C}+2\pi f_s C_1 v_{C1S}=0 \end{cases} \tag{6}$$

In the (6) , i_{gs}, i_{gc} and v_{gs}, v_{gc} respectively represent the amplitude of the sine and cosine components of the current and voltage during steady state operation. The working frequency is f_s ; $\omega_s = 2\pi f_s$; $R_{ac} = 8n^2 R_{eq} / \pi^2$;Where, the resonant current i_g and resonant voltage v_g are in a steady state.

Without considering the influence of parasitic parameters, the DC voltage gain G of the CLLLC converter when it is running forward can be obtained:

$$\left|G(jw)\right| = 4\sqrt{2}\pi^2 R_{ac} f_s^{\,2} L_m C_1 \sin\left(\frac{\pi}{2}d\right) \Big/ n\sqrt{\left[R_{ac}\left(4\pi^2 f_s^{\,2} L_e C_1 - 1\right)\right]^2 + \left[2\pi f_s L_m \left(1 - 4\pi^2 f_s^{\,2} L_1 C_1\right)\right]^2} \tag{7}$$

Type $L_e = L_1 + L_{\mathrm{m}}$, duty ratio d take 0.5, a resonant frequency as follows: $f_r = \frac{1}{2\pi\sqrt{L_1 C_1}}$;The normalized frequency: $f_n = \frac{f_s}{f_r}$; $R_{ac} = 8n^2 R_{eq} / \pi^2$;Excitation inductance and the ratio of resonant inductance coefficient as follows: $K = \frac{L_m}{L_1}$;Quality factor is: $Q = \frac{2\pi f_r L_1}{R_{ac}}$ .Substitute it into (7) to get:

$$\left|G(jw)\right| = \frac{2\sqrt{2}k f_n^{\,2}}{n\sqrt{\left[(1+k) f_n^{\,2} - 1\right]^2 + \left[Q f_n \left(f_n^{\,2} - 1\right)\right]^2}} \tag{8}$$

4. Parameter design of CLLLC resonant converter

The resonant cavity parameters of the CLLLC resonant converter are designed by the fundamental equivalent circuit. The following steps are taken:

(1) Determine the input and output indexes;

(2) Select the resonant frequency at work;

(3) Calculate the transformer ratio and resonant element values;

(4) Analyze the voltage gain curve

Table 1. The parameters of CLLLC resonant converter

Project	Parameter
Input voltage range	$V_{in\max} = 1150;\ V_{in\min} = 850$
Rated input voltage	$V_{inNom} = 1000$
Rated output voltage	$V_{out} = 380$
The output power	$P_0 = 20kW$
Resonant frequency	$f_r = 10kHz$
Rated input/output operating frequency	Operating at the resonaut frequency f_r

Based on the analysis of the fundamental equivalent circuit of the CLLLC resonant converter, the parameters of the secondary side are designed to be converted to the value equal to the resonant element of the primary side to ensure the complete symmetry of the topology of the converter.

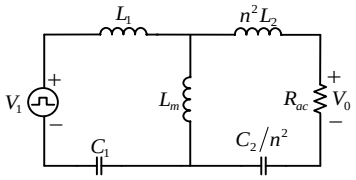

Figure 3. CLLLC resonant converter fundamental wave equivalent model

According to the basic equivalent circuit DC voltage gain, the voltage, current, power and resonant frequency are known. The desired maximum voltage gain value can be obtained simply, and the normalized gain curve can be derived accordingly. A resonant frequency for: $f_r = \frac{1}{2\pi\sqrt{L_1C_1}}$;The normalized frequency: $f_n = \frac{f_s}{f_r}$; $R_{ac} = 8n^2R_{eq}/\pi^2$;Excitation inductance and the ratio of resonant inductance coefficient as follows: $K = \frac{L_m}{L_1}$;Quality factor is: $Q = \frac{2\pi f_r L_1}{R_{ac}}$.That is:

$$\left|G(jw)\right| = \frac{kf_n^{\,2}}{\sqrt{\left[(1+k)\,f_n^{\,2}-1\right]^2+\left[Qkf_n\left(f_n^{\,2}-1\right)\right]^2}} \tag{9}$$

Transformer ratio:

$$n = \frac{V_{inNom}}{V_{out}} = 2.6 \tag{10}$$

Maximum and minimum voltage gain:

$$\begin{cases} G_{\min} = n * \dfrac{V_0 + V_d}{V_{in\max}} = 0.86 \\ G_{\max} = n * \dfrac{V_0 + V_d}{V_{in\min}} = 1.16 \end{cases} \tag{11}$$

where, V_d is the pressure drop of the switch tube.

Calculation of equivalent load electric and reflection resistance at the output end:

$$\begin{cases} R_{eq} = \dfrac{V_{out}^{\,2}}{P_0} = \dfrac{380^2}{20kW} = 7.22\Omega \\ \mathrm{R}_{ac} = n^2 \dfrac{8}{\pi^2}\dfrac{V_{out}^{\,2}}{P_0} = 39.56\Omega \end{cases} \tag{12}$$

Take excitation inductance and the ratio of resonant inductance for 3 or $K = 3$;Calculate the quality factor:

$$Q = \frac{0.95}{k * G_{\max}} * \sqrt{k + \frac{G_{\max}^{\,2}}{G_{\max}^{\,2}-1}} = 0.717 \tag{13}$$

Minimum and maximum operating frequency range of the converter:

$$\begin{cases} R_{eq} = \dfrac{V_{out}^{\,2}}{P_0} = \dfrac{380^2}{20kW} = 7.22\Omega \\ \mathrm{R}_{ac} = n^2 \dfrac{8}{\pi^2}\dfrac{V_{out}^{\,2}}{P_0} = 39.56\Omega \end{cases} \tag{14}$$

The calculated resonant element parameters are as follows:

$$\begin{cases} C_1 = \dfrac{1}{2\pi f_r R_{ac} Q} = 561nF \\ L_1 = \dfrac{QR_{ac}}{2\pi f_r} = 451\mu H \\ C_2 = n^2 C_1 = 3.79\mu F \\ L_2 = \dfrac{L_1}{n^2} = 66.72\mu H \end{cases} \tag{15}$$

Under different quality factors and normalized frequency, the DC voltage gain of CLLLC resonant converter is shown in Figure 4:

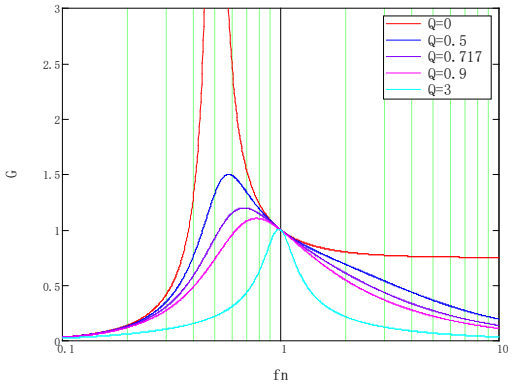

Figure 4. Gain curve of CLLC converter with different Q

Take $K = 3$ under different quality factor, the normalized frequency f_n CLLLC resonant converter and dc voltage gain G curve as shown in Figure 4. $Q = 0$ represents no-load DC gain. In order to obtain greater voltage gain, the actual operating frequency of the converter should be less than the resonant frequency. On the premise of satisfying ZVS and ZCS, try to choose the quality factor with larger gain. Normalized frequency f_n, namely, the ratio between series resonant inductor L_1 and excitation inductor L_m, should not be too large, and f_n generally takes a value of 2.5-6.

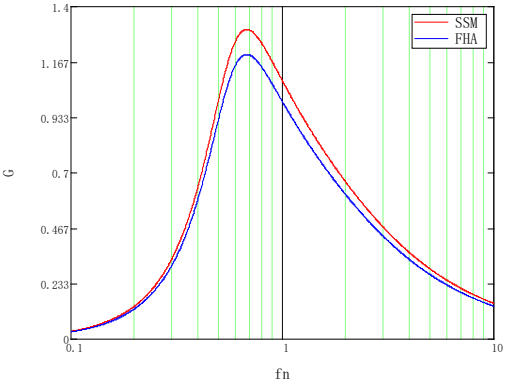

Figure 5. Gain curve of FHA and SSM with same Q

By Figure 5, you can see that under the same conditions of dc voltage gain contrast: based on the FHA dc voltage gain curve is deduced and the extension is used to describe function is deduced from the fit of the model of dc voltage gain, same said extension describing function model of right, based on extended description function of dc voltage gain value using FHA model error is small.

5. Small signal perturbation model analysis of CLLLC resonant converter

Assuming that CLLLC is in stable operation state, the transfer function of small signal model is deduced by adding small signal perturbation to large signal model. The small signal perturbation of CLLLC resonant converter can be expressed as $v_1=V_1+\hat{v}_1$、$f=f_s+\hat{f}_s$、$i_{ms}=i_{mS}+\hat{i}_{ms}$、$d=D+\hat{d}$、$i_{mc}=i_{mC}+\hat{i}_{mc}$ $i_{ms}=i_{mS}+\hat{i}_{ms}$、$i_{1c}=i_{1C}+\hat{i}_{1c}$、$i_{1s}=i_{1S}+\hat{i}_{1s}$、$v_{C1c}=v_{C1C}+\hat{v}_{C1c}$、$v_{C1s}=v_{C1S}+\hat{v}_{C1s}$、$v_{C2c}=v_{C2C}+\hat{v}_{C2c}$、$v_{C2s}=v_{C2S}+\hat{v}_{C2s}$.

The small signal perturbation is brought into the steady-state solution of the large signal, and the influence of the infinite small amount is ignored, and the small signal model of the CLLLC resonant converter is obtained, namely:

$$L_1\frac{d\hat{i}_{1s}}{dt}=A_1\hat{i}_{ic}+B_{1s}\hat{f}-\hat{v}_{C1s}-2K_s\hat{v}_0-G_{pis}\left(\hat{i}_{1s}-\hat{i}_{ms}\right)+G_{ps}\left(\hat{i}_{1c}-\hat{i}_{mc}\right)+K_v\hat{v}_1 \tag{16}$$

$$L_1\frac{d\hat{i}_{1c}}{dt}=-A_1\hat{i}_{is}-B_{1c}\hat{f}-\hat{v}_{C1c}-2K_c\hat{v}_0-G_{pic}\left(\hat{i}_{1c}-\hat{i}_{mc}\right)+G_{pc}\left(\hat{i}_{1s}-\hat{i}_{ms}\right) \tag{17}$$

$$L_m\frac{d\hat{i}_{ms}}{dt}=A_m\hat{i}_{mc}+B_{ms}\hat{f}-2K_s\hat{v}_0+G_{pis}\left(\hat{i}_{1s}-\hat{i}_{ms}\right)-G_{ps}\left(\hat{i}_{1c}-\hat{i}_{mc}\right) \tag{18}$$

$$L_m\frac{d\hat{i}_{mc}}{dt}=-A_m\hat{i}_{ms}+B_{mc}\hat{f}-2K_c\hat{v}_0+G_{pic}\left(\hat{i}_{1c}-\hat{i}_{mc}\right)-G_{pc}\left(\hat{i}_{1s}-\hat{i}_{ms}\right) \tag{19}$$

$$C_1\frac{d\hat{v}_{C1s}}{dt}=\hat{i}_{1s}+G_{1s}\hat{v}_{C1c}+H_c\hat{f} \tag{20}$$

$$C_1\frac{d\hat{v}_{C1c}}{dt}=\hat{i}_{1c}+G_{1s}\hat{v}_{C1s}+H_s\hat{f} \tag{21}$$

$$C_0\frac{d\hat{v}_{C0}}{dt}=\frac{K_s\left(\hat{i}_{1s}-\hat{i}_{ms}\right)+K_c\left(\hat{i}_{1c}-\hat{i}_{mc}\right)-R_{eq}\hat{v}_{C0}}{R_x} \tag{22}$$

Type in the $A_1=2\pi f_sL_1$; $A_m=2\pi f_sL_m$; $B_{1s}=2\pi L_1i_{1c}$; $B_{1c}=2\pi L_1i_{1s}$; $B_{ms}=2\pi L_mi_{mc}$; $B_{mc}=2\pi L_mi_{ms}$; $G_{1s}=G_{1c}=2\pi f_sC_1$; $G_{2s}=G_{2c}=2\pi f_sC_2$; $H_c=C_1v_{C1c}$; $H_s=C_1v_{C1s}$; $K_s=\frac{2n\left(i_{1s}-i_{ms}\right)}{\pi X_i}$; $K_c=\frac{2n\left(i_{1c}-i_{mc}\right)}{\pi X_i}$; $J_s=C_2v_{C2c}$; $J_c=C_2v_{C2s}$; $G_{pis}=-\frac{4n\left(i_{1c}-i_{mc}\right)^2v_0}{\pi X_i^3}$; $G_{pic}=\frac{4n\left(i_{1s}-i_{ms}\right)^2v_0}{\pi X_i^3}$; $G_{V0}=\frac{4n\left(i_{1c}-i_{mc}\right)}{\pi X_i}$; $H_{V0}=\frac{4n\left(i_{1s}-i_{ms}\right)}{\pi X_i}$; $G_{pc}=-\frac{4n\left(i_{1s}-i_{ms}\right)\left(i_{1c}-i_{mc}\right)v_0}{\pi X_i^3}$; $G_{ps}=\frac{4n\left(i_{1s}-i_{ms}\right)\left(i_{1c}-i_{mc}\right)v_0}{\pi X_i^3}$; $R_x=\frac{R_{eq}}{R_{eq}+r}$.

The small-signal model of the output voltage obtained by sorting out the above of state is:

$$\hat{V}_0=K_sR'\left(\hat{i}_{1s}-\hat{i}_{ms}\right)+K_cR'\left(\hat{i}_{1c}-\hat{i}_{mc}\right)+\frac{R'}{r}\hat{v}_{C0} \tag{23}$$

The frequency is taken as the input variable and the output variable as the voltage disturbance small signal. The design parameters of CLLLC are substituted into the small-signal model expression, and the above small-signal model is expanded to obtain the transfer function of the influence of switching frequency on voltage:

$$G(s)=\frac{\hat{v}_0(s)}{\hat{f}(s)} \tag{24}$$

6. Simulation verification

The calculated resonant parameters were simulated under the PSIM simulation software when the CLLLC resonant converter was running forward. The resonant frequency was set as 10kHz, and the simulation results were shown in Figure 6

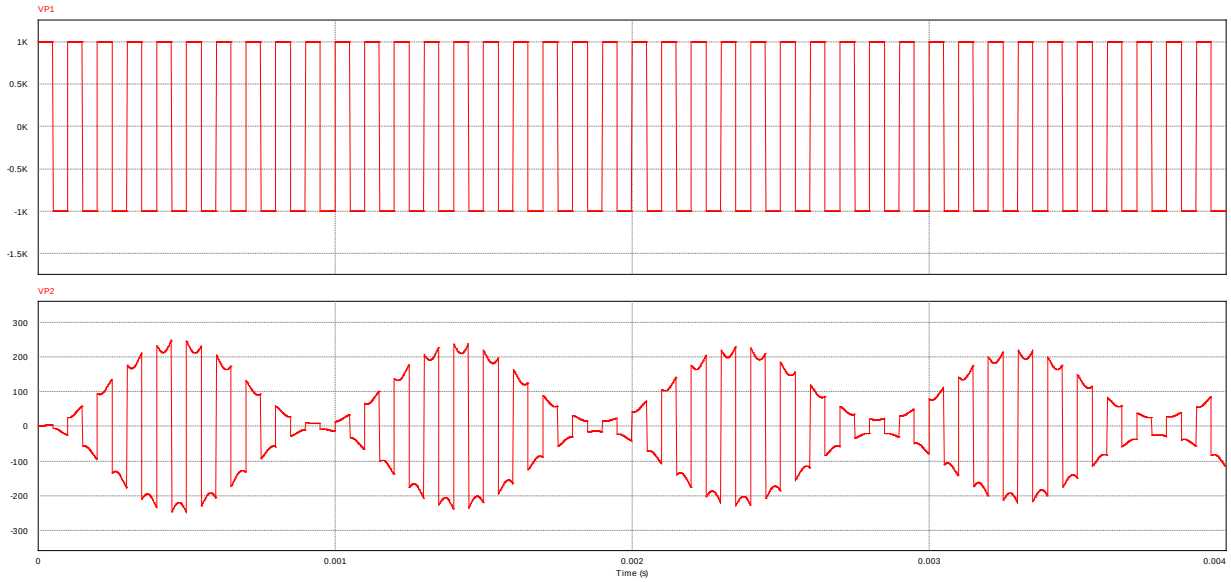

Figure 6. Input voltage and output voltage curve of CLLLC resonant converter

As can be seen from Figure 6, the output voltage of the inverter side V_{p1} is 50% duty cycle, 1000V high-frequency square wave voltage, through the resonator and the output voltage of the high-frequency transformer, is a high-frequency sine wave. Figure 7 is a schematic diagram of the resonant current. The current is in phase with the output voltage of the resonator, which ensures the soft switching characteristics and reduces eddy current loss.

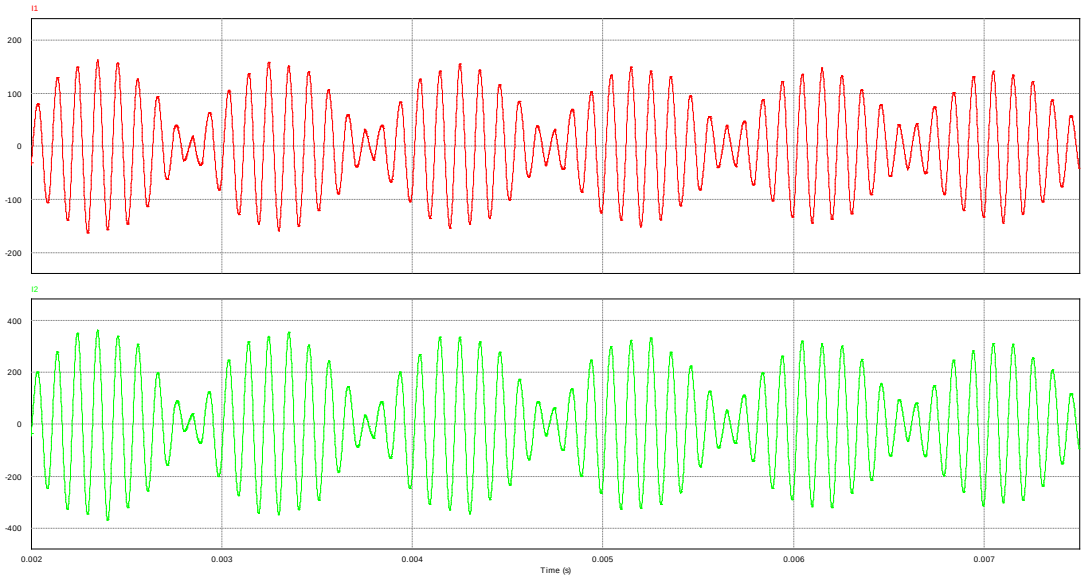

Figure 7. Input voltage and output voltage curve of CLLLC resonant converter

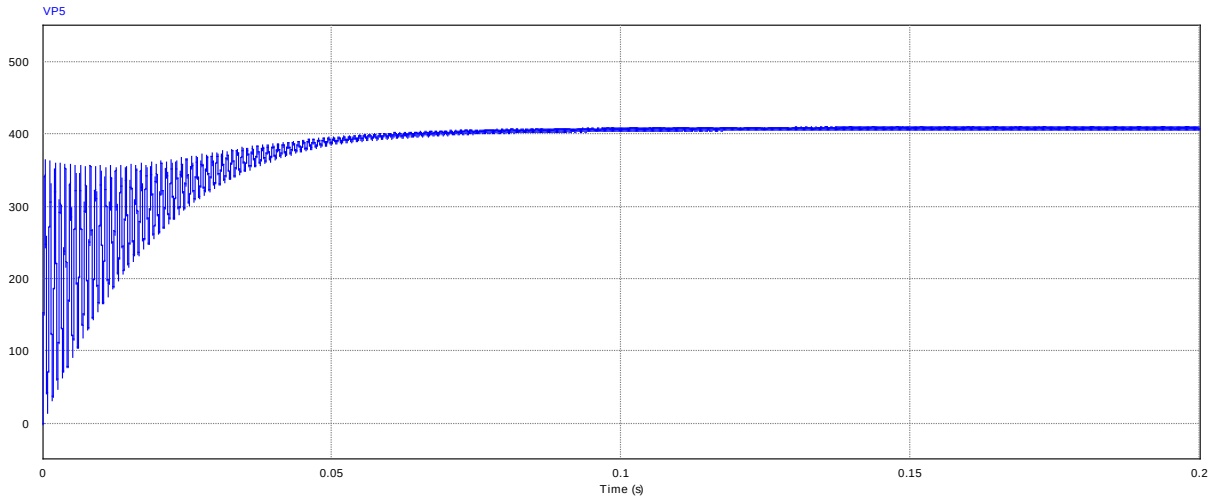

Figure 8. Output voltage curve of CLLLC resonant converter

When the CLLLC resonant converter is running forward, the rated output voltage is shown in Figure8, and the voltage can finally stabilize at 380V.The results are consistent with the above calculation results, which verifies the correctness of the design

7. Conclusion

In this paper, the extended description function method is used to establish the large-signal steady-state model of the forward operation of CLLLC, and the small-signal perturbation is added to the steady-state solution of the large-signal model to obtain the small-signal model of the CLLLC resonant converter. Mathcad software was used to compare the voltage gain and the gain of the equivalent model of fundamental wave, and the application of the extended description function method was verified. The resonant cavity design of 20kW/1000V/380VCLLLC resonant converter is completed, and the forward operation of CLLLC is simulated and verified by PSIM simulation software. The simulation results show that the model and the design parameters are correct, which provides a new idea for the practical application of CLLLC resonant converter and the design of feedback compensator.

8. Reference

[1] J. Z. Liu. “Basic issues of the utilization of large-scale renewable power with high security and efficiency.” Proceedings of the CSEE, 2013,33(16):1-8.
[2] M. Ding, W. S. Wang, X. L. Wang. “A review on the effect of large-scale PV generation on power systems.” Proceedings of the CSEE,2014, 34(1): 2-14. (in Chinese)
[3] C. X. Li, J. Wang, X. M. Ye, Q. Yu. “Development and prospects of new energy in China.” Electric Power Science and Engineering, 2012, 28(4):1-8.
[4] S. M. Tian, W. P. Luan, D. X. Zhang , C. H. Liang,Y. J. Sun. “Technical forms and key technologies on energy internet.” Wind Energy Industry(No.2,2016).China Agricultural Machinery Industry Association Wind Machinery Branch ,2016:24-37.
[5] G. P. Chen, M..J. Li, T. Xu, M S.Liu.“Study on technical bottleneck of new energy development.” Proceedings of the CSEE, 2017,37(1): 20-26.
[6] Q. Song, B. Zhao, W. H. Liu, R. Zeng.“An overview of research on smart DC distribution power network.” Proceedings of the CSEE, 2013,33(25):9-19+5.
[7] T. Y. Jiang.“Research on the bidirectional resonant DC/DC converter.” Zhejiang University,2015.
[8] B. Zhao, Q. G. Yu, W. X. Sun.“Bi-directional full-bridge DC-DC converters with dual-phase-shifting control and lts backflow power characteristic analysis.” Proceedings of the CSEE,2012,32(12):43-50.

[9] D. Dujic,C. H. Zhao,A. Mester et al., "Power electronic traction transformer-low voltage prototype." in IEEE Transactions on Power Electronics, vol. 28, no. 12, pp. 5522-5534, Dec. 2013.
[10] A. Pawellek, C. Oeder and T. Duerbaum, "Comparison of resonant LLC and LCC converters for low-profile applications." Proceedings of the 2011 14th European Conference on Power Electronics and Applications, Birmingham, 2011, pp. 1-10.
[11] Y. Y. Cai."Research on high frequency isolated bidirectional resonant DC-DC converters." China University of Mining and Technology (Beijing),2015.
[12] J. Li"Research on wide voltage range resonant bidirectional DC/DC converter." Harbin Institute of Technology,2019.
[13] Y. L. Li. "A research of bidirectional power converter for electric vehicle." University of Electronic Science and Technology of China,2019.
[14] W. Chen, Z. Y.Lu."Investigation on set of quasi-isomorphic topologies and structural variations of type-4 LLC resonant DC-DC converter based on module function identification." Proceedings of the CSEE,2009,29(09):35-42.
[15] A. Sankar, A. Mallik and A. Khaligh, "Extended harmonics based phase tracking for synchronous rectification in CLLC converters." in IEEE Transactions on Industrial Electronics, vol. 66, no. 8, pp. 6592-6603, Aug. 2019.
[16] Q. C. Chen. "Research on key technologies of bidirectional CLLLC resonant DC/DC converter." Harbin Institute of Technology,2015.
[17] L. Zhu, "A novel soft-commutating isolated boost full-bridge ZVS-PWM DC-DC converter for bidirectional high power applications." 2004 IEEE 35th Annual Power Electronics Specialists Conference (IEEE Cat. No.04CH37551), Aachen, Germany, 2004, pp. 2141-2146 Vol.3.
[18] J. X. Zhang. "Research on design and control method of CLLC resonant isolated bidirectional DC/DC converter." Xi 'an University of Technology,2019.
[19] J. Jung, H. Kim, M. Ryu and J. Baek, "Design methodology of bidirectional CLLC resonant converter for high-frequency isolation of DC distribution systems." in IEEE Transactions on Power Electronics,vol.28,no.4,pp.1741-1755,April 2013.
[20] L. Zhao, Y. Q. Pei, X. H. Liu, W J. Fan, Y. Du. "Design methodology of CLLC resonant converters for electric vehicle battery chargers." Proceedings of the csee:1-14 [2020-07-07].
[21] S. C. Li, B. Y. Liu, Q. Jiang, S. X. Duan. "Performance analysis of bidirectional CLLLC resonant converter with synchronous PWM control strategy." Transactions of China Electrotechnical Society, 2019,34(S2):543-552.
[22] Y. H.Jiang,L.W. Shuai,Q.N. Wu, Y. L. Cao."Optimization of resonance parameter for output port of bi-directional electronic transformer based on quantum particle Swarm." Automation of Electric Power Systems,2020,44(11):171-190.
[23] Y. J. Liu,G. P. Du,X. Y. Wang,Y. X. Lei. "Analysis and design of high-efficiency bidirectional GaN-based CLLC resonant converter." MDPI, 2019,12(20).
[24] K. Sun, H. Chen, H. F. Wu. "A review of analysis method and control technology for isolated bidirectional DC-DC converter used in energy storage systems." New Technology of Electrical Power,2019,38(08):1-9.
[25] L. N.Zhan. "Modeling of LLC resonant converter based on extended describing function method." Qingdao University,2014.
[26] F. Y. Zhang. "Optimization control and design of bidirectional full-bridge LLC resonant converter." Shandong University,2019.
[27] S. C. Zheng, S. M. Liu, J. Wang, "CLLLC resonant bidirectional full-bridge DC-DC converter." Journal of Electromechanical Systems and Its Automatics,2019,31(04):83-90.

Acknowledgements

This research was supported by the kjcb-2020-34 program through the State Grid Hebei Electric Power Co., Ltd project.